

# Hard Diffraction in Vector Meson Production at HERA

P. MARAGE

*Université Libre de Bruxelles - CP 230, B-1050 Brussels, Belgium*  
*E-mail: pmarage@ulb.ac.be*

A review is presented of diffractive vector meson production at HERA, with stress on the investigation of “hard” features and comparisons with theoretical predictions based on perturbative QCD approaches.<sup>a</sup>

<sup>a</sup>Paper presented at the XXIIIth International Symposium on Multiparticle Dynamics, Delphi, Greece, September 1998.

## 1 Introduction

Since the first data taking in 1992, the HERA high energy  $ep$  collider has shown to be a powerful tool for the study of the strong interaction, in particular to test the domain of applicability and the relevance of several approximations of perturbative QCD (pQCD) in the field of diffraction.

### 1.1 Total Cross Section and Diffraction

Two major experimental discoveries were made at HERA for the understanding of strong interactions and of hadron structure.

First, the observation that, in the deep inelastic scattering (DIS) domain, the  $\gamma^*p$  cross section increases rapidly with energy. This is attributed to an enhancement of the number of gluons in the proton, the gluon structure function  $x \cdot G(Q^2, x)$  thus growing fast as  $x$  decreases ( $x$  is the Bjorken scaling variable:  $x = Q^2/2p \cdot q$ , where  $p$  and  $q$  are, respectively, the proton and the intermediate photon four-momenta and  $Q^2 = -q^2$ ; the  $\gamma^*p$  centre of mass energy  $W$  is given by  $W^2 = Q^2/x - Q^2$ ).

This “hard” behaviour differs from that of the total and the elastic hadron-hadron cross sections (closely related through the optical theorem), which are characterised by a “soft” energy dependence. In the framework of Regge theory<sup>1</sup>, elastic scattering is attributed at high energy to the exchange between the incoming hadrons of a colourless object, the pomeron  $\mathbb{P}$ . The energy dependence of the total cross section is proportional to  $W^{2[1-\alpha_{\mathbb{P}}(t)]}$ , where the pomeron trajectory  $\alpha_{\mathbb{P}}(t)$  is parameterised as<sup>2,3</sup>

$$\alpha_{\mathbb{P}}(t) = \alpha_{\mathbb{P}}(0) + \alpha' \cdot t \simeq 1.08 + 0.25 t, \quad (1)$$

$t$  being the square of the four-momentum transfer.

The second major discovery in DIS at HERA is the substantial contribution (8 – 10%) of events formed of two hadronic subsystems separated by a large gap in rapidity, devoid of hadronic activity<sup>4</sup>.

This process is similar to diffractive scattering in hadron-hadron interactions, where the incoming hadrons are excited without colour exchange. Diffraction thus forms an extension of elastic scattering and is dominated at high energy by pomeron exchange with the “soft” behaviour of eq. (1). The interesting feature at HERA was to observe diffraction as a leading twist process in DIS.

### 1.2 “Soft” Vector Meson Production

An important case of diffractive scattering is that of vector meson (VM) production, in particular when the proton remains intact in the reaction:  $e + p \rightarrow e + p + VM$ .

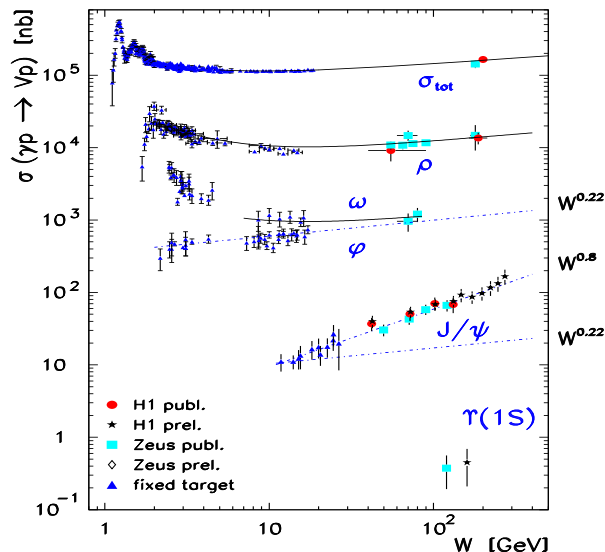


Figure 1: Total photoproduction and VM photoproduction cross sections, for fixed target and HERA experiments. The solid curves are obtained from the “soft” pomeron parameterisation<sup>2</sup>, with a decreasing contribution of reggeon exchange at low energy; the energy dependence noted  $W^{0.22}$  is obtained from eq. (1), taking into account the  $t$  distribution of the events. The “hard”,  $W^{0.8}$ , dependence is also shown in the case of  $J/\psi$  photoproduction.

In the vector meson dominance (VDM) approach, the  $J^{PC} = 1^{--}$  photon is modelled as the superposition of the lightest VM’s ( $\rho$ ,  $\omega$ ,  $\phi$ ). The total  $\gamma p$

cross section is thus expected to present the characteristic “soft” behaviour of hadron-hadron interactions. The production of light VM’s, which is directly related to elastic scattering (with a differential absorption by the target proton of some of the hadronic components of the photon) is also expected to present a “soft” energy dependence. The gross features of this interpretation are supported by a huge quantity of data accumulated by fixed target experiments<sup>5,6,7,8</sup>. At high energy, the HERA experiments have measured the total cross section in photoproduction ( $Q^2 \approx 0$ )<sup>9,10</sup> and the cross section for diffractive photoproduction of  $\rho$ <sup>11,12,13,14</sup>,  $\omega$ <sup>15</sup>,  $\phi$ <sup>16</sup>. They exhibit the “soft” energy dependence described by parameterisation (1), as shown on Fig. 1 (at low energy, a contribution from reggeon exchange, decreasing with  $W$ , is present for  $\sigma_{tot}$ ,  $\rho$  and  $\omega$ ). The  $W$  dependence of  $\rho$  photoproduction, studied as a function of  $t$ , has also allowed measuring the slope  $\alpha'$  of the pomeron trajectory<sup>17</sup>.

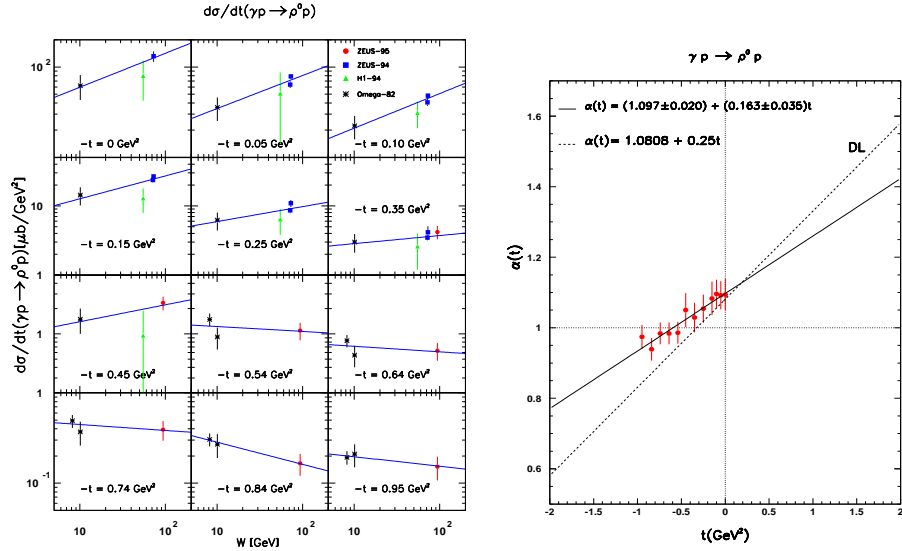


Figure 2: a)  $W$  dependence of  $\rho$  meson photoproduction, in several bins in  $t$ <sup>17</sup>. b) Slope of the pomeron trajectory for the reaction  $\gamma p \rightarrow \rho p$  as obtained from a); the dotted curve represents the parameterisation of 2.

### 1.3 “Hard” Vector Meson Production and QCD

At HERA, the main interest is for the production of light VM’s at high  $Q^2$  or high  $|t|$ , and for the production of heavy vector mesons. This is because two far-reaching questions can be raised:

1. Is the “soft”, hadron-like behaviour observed in light VM photoproduction also observed in the presence of a “hard” scale: high  $Q^2$ , high  $|t|$  or large quark mass ( $c$ ,  $b$ ) ?

2. In the presence of a “hard” scale, what are the relevant assumptions and approximations in pQCD calculations required to describe diffractive VM production ? Can this shed light on the partonic nature of the pomeron ?

A large number of experimental studies have thus been performed at HERA to investigate these questions. Data have been collected, in the presence of the scales  $Q^2$ ,  $m_q$  and  $t$ , on the production of  $\rho$ ,  $\omega$ ,  $\phi$ ,  $\rho'$ ,  $J/\psi$ ,  $\psi(2s)$  and  $\Upsilon$  mesons, with studies of the differential  $Q^2$ ,  $W$  and  $t$  distributions, of the polarisation characteristics, of the cross section ratio between several VM production and of the mass shape. Only a small fraction of these results will be presented here. They are largely based on results presented at the 29th Int. Conf. on HEP held at Vancouver, Canada, in July, 1998.

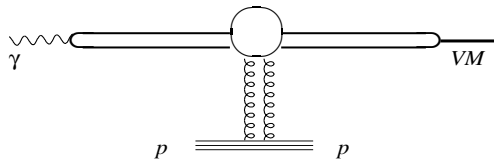


Figure 3: Schematic representation of VM production in pQCD.

A large number of theoretical papers based on pQCD has also been published, presenting predictions for VM production under various assumptions and approximations (see e.g. <sup>18,19,20,21,22,23,24</sup>). A general feature of these approaches is that, at high energy, the amplitude is factorised in three contributions, characterised by very different time scales (see Fig. 3):

$$A = \Psi_{\gamma^* \rightarrow q\bar{q}}^* \otimes M_{q\bar{q}+p \rightarrow q\bar{q}+p} \otimes \Psi_{q\bar{q} \rightarrow V}. \quad (2)$$

The first factor corresponds to the amplitude for a long distance fluctuation of the photon into a  $q\bar{q}$  pair. The second factor describes the (short-time) scattering amplitude of this hadronic state with the proton. The exchange is generally modelled as a gluon pair (i.e. a colour singlet system), with  $M \propto |x \cdot G(K^2, x)|^2$ , the square of the gluon density in the proton. The order of magnitude of the scale  $K^2$  at which the gluon structure function is probed is  $K^2 \simeq 1/4 (Q^2 + m_V^2 + |t|)$ , since these three variables contribute to the “resolution” of the process; the factor 1/4 comes from the sharing of the momenta between the two quarks. The third factor in eq. (2) accounts for the recombination of the scattered hadronic state in the VM wave function.

However, as stressed e.g. in <sup>21</sup>, theoretical calculations are affected by significant uncertainties concerning the choice of the QCD scale, of the gluon

distribution and of the VM wave function, in particular the effects of Fermi motion of the quarks within the meson.

## 2 Differential Distributions

### 2.1 $W$ Dependence

The most striking manifestation of pQCD features in VM production is to be expected in the  $W$  dependence of the cross section, since the latter is related to the square of the gluon density in the proton, which increases rapidly with  $W$  in the presence of a hard scale.

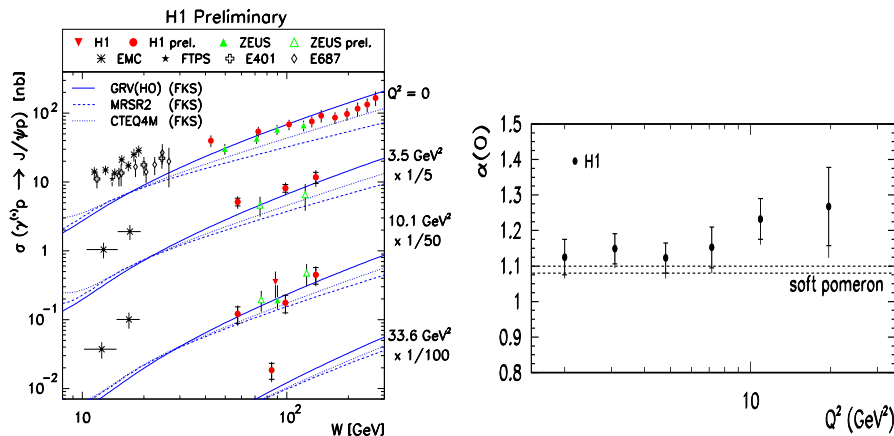


Figure 4: a)  $W$  dependence of  $J/\psi$  meson photo- and electroproduction; the curves represent predictions of a pQCD model<sup>21</sup> for different gluon distribution functions in the proton and  $m_c = 1.5 \text{ GeV}$ <sup>28</sup>. b)  $Q^2$  dependence of the intercept  $\alpha_P(0)$  for  $\rho$  meson electroproduction<sup>30</sup>; the dashed lines represent the range of values for the “soft” pomeron intercept, as derived from fits to the total and elastic hadron-hadron cross section measurements<sup>2,3</sup>.

A “hard” behaviour is observed in photoproduction of  $J/\psi$  mesons<sup>26,25,27</sup>, as shown in Figs. 1 and 4a. When the  $W$  dependence of the cross section is parameterised as  $\propto W^\delta$  (in a Regge approach,  $\delta = 4\alpha_P(\langle t \rangle)$ ), one finds  $\delta \simeq 0.8$  for  $J/\psi$  photoproduction. The contrast is thus manifest with the “soft” behaviour of light VM photoproduction, for which  $\delta = 0.20 - 0.25$  (this value is in agreement with the parameterisation of eq.(1), taking into account the  $t$  distribution). A similar behaviour is observed for  $J/\psi$  electroproduction<sup>28,29</sup> (Fig. 4a). The curves on this figure represent the predictions of a model based on pQCD calculations<sup>21</sup>, for different parameterisations of the gluon distribution in the proton. The agreement of these predictions with the

data, especially as to the shape of the distribution (the absolute values are sensitive to the input charm quark mass), supports the modelisation of the pomeron as a colour-singlet gluon pair.

For  $\rho$  and  $\phi$  meson electroproduction, the “hard” scale is related to  $Q^2$ . Although the precision of the data is still limited, an indication is present of a steeper  $W$  dependence of the  $\gamma^*p$  cross section as  $Q^2$  increases for the  $\rho$ <sup>29,30</sup> and for the  $\phi$ <sup>31</sup>. This is shown for the  $\rho$  on Fig. 4b, where the pomeron intercept  $\alpha_P(0)$  is plotted.

## 2.2 $Q^2$ Dependence

The cross section for  $\rho$  production in the DIS domain is presented as a function of  $Q^2$  on Fig. 5a for the ZEUS<sup>29</sup> and H1<sup>30</sup> experiments, which are in agreement. The  $Q^2$  dependence is well parameterised in this domain as  $d\sigma/dQ^2 \propto 1/(Q^2 + m_V^2)^n$ , with  $n \simeq 2.28 \pm 0.06$  (combined value). This behaviour is expected from pQCD calculations, which give for the (dominant - see below) longitudinal cross section<sup>20</sup>:  $\sigma_L \propto [\alpha_s(Q^2) \cdot xG(Q^2, x)]^2/Q^6$ , when taking into account the  $Q^2$  dependence in  $\alpha_s(Q^2)$  and in  $xG(Q^2, x)$ , as well as other uncertainties affecting the calculations<sup>21</sup>. Over the full measurement range, including photoproduction, the  $Q^2$  dependence of  $\rho$  cross section is best described by the QCD based model of ref.<sup>24</sup>.

For  $\phi$  production<sup>31</sup>, a value similar to that for the  $\rho$  is found. For  $J/\psi$  production, the values  $n = 2.24 \pm 0.19$ <sup>28</sup> and  $n = 1.58 \pm 0.25$ <sup>29</sup> are obtained.

## 2.3 $t$ Dependence

For not too large  $|t|$  values, the  $t$  distribution of VM production can reasonably well be parameterised in the exponential form  $d\sigma/dt \propto e^{-b|t|}$ . In an optical model approach of diffraction, the slope parameter  $b$  is related to the convolution of the sizes of the interacting objects:  $b \propto R_p^2 + R_{q\bar{q}}^2$ , with the proton radius  $R_p$  giving a contribution of the order of  $4 - 5 \text{ GeV}^{-2}$ .

As observed in Fig. 5b, the slope  $b$  for  $\rho$  production decreases when  $Q^2$  increases, in agreement with the decrease of the transverse size of the virtual  $q\bar{q}$  pair expected in pQCD calculations.

For  $J/\psi$  photo- and electroproduction, a slope of the order of  $b \simeq 4 - 5 \text{ GeV}^{-2}$  is measured<sup>25,26,29,28</sup>, confirming the small size of the  $J/\psi$  meson.

Fig. 5b also suggests that, at low  $Q^2$ , the slope parameter  $b$  for  $\rho$  production increases from the fixed target to the HERA energy range. This behaviour, known as “shrinkage” and expected in Regge theory, is related to the non-zero slope  $\alpha'$  of the “soft” pomeron trajectory. In contrast, no shrinkage is expected in a pQCD approach for asymptotically high values of the QCD scale ( $\alpha' \approx 0$ ).

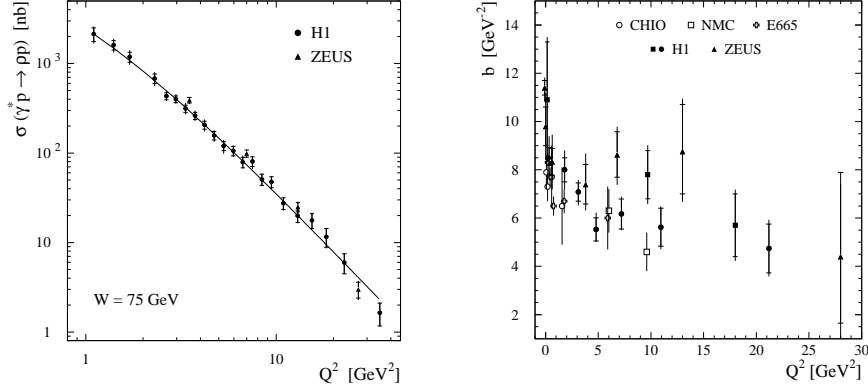


Figure 5: a)  $Q^2$  dependence of  $\rho$  production cross section<sup>29,28</sup>; the superimposed curve is for  $n = 2.24$ . b)  $Q^2$  dependence of the slope parameter  $b$  for elastic  $\rho$  production: fixed target measurements of ref.<sup>6,7,8</sup> and HERA measurements of ref.<sup>29,32,30</sup>.

However, no significant measurement has been possible so far using the HERA experiments only, neither for  $\rho$  production at high  $Q^2$  nor for  $J/\psi$  production, and the conclusions to be drawn from comparisons between fixed target and HERA data remain controversial<sup>17,33</sup>.

### 3 Polarisation

The measurement of VM decay angular distributions allows the determination of the spin density matrix elements, which are related to the helicity amplitude  $T_{\lambda_V \lambda_\gamma}$ , where  $\lambda_V$  and  $\lambda_\gamma$  are the helicities of the VM and of the photon, respectively<sup>34</sup>. In the case of  $s$ -channel helicity conservation (SCHC), the helicity of the photon is retained by the VM and the matrix elements containing helicity changing amplitudes ( $\lambda_V \neq \lambda_\gamma$ ) are thus zero.

Measurements of the full set of matrix elements have been performed for  $\rho$  as a function of  $Q^2$  (Fig. 6a),  $W$  and  $t$ <sup>30,35</sup>, and for  $\phi$  mesons<sup>35</sup>.

As is visible on Fig. 6, the data are compatible with SCHC, except for a small but significant deviation from zero of the matrix element  $r_{00}^5$ . The helicity flip amplitude  $T_{\lambda_\rho \lambda_\gamma} = T_{01}$  is thus determined to be  $8 \pm 3\%$  of the non-flip amplitudes  $\sqrt{T_{00}^2 + T_{11}^2}$ . This value is of the order of magnitude of that found at lower energy and lower  $Q^2$ <sup>6,36</sup>.

Neglecting the small violation of SCHC (which would affect the value of  $R$  by  $2.5 \pm 1.5\%$ ), the matrix element  $r_{00}^{04}$  can be used to extract the ratio  $R$  of cross sections for  $\rho$  production by longitudinal and transverse virtual photons:  $R = \sigma_L / \sigma_T = r_{00}^{04} / \varepsilon \cdot (1 - r_{00}^{04})$ , where  $\varepsilon$  is the polarisation parameter ( $\langle \varepsilon \rangle = 0.99$  at HERA). Fig. 6b shows that  $R$  rises steeply at small  $Q^2$ , and

that the longitudinal  $\gamma^*p$  cross section dominates over the transverse cross section for  $Q^2 \gtrsim 2 \text{ GeV}^2$ . However, the rise is non-linear, with a weakening dependence at large  $Q^2$  values, and  $R$  is  $\approx 3$  for  $Q^2 \gtrsim 10 - 20 \text{ GeV}^2$ .

This feature is not reproduced by numerous models based on VDM or QCD, which predict a linear increase of  $R$  with  $Q^2$ . However, the model of ref. <sup>24</sup>, based on QCD, gives a good description of  $R$  over the full  $Q^2$  range, as does also a model based on GVDM <sup>37</sup>. Another model based on QCD <sup>22</sup> predicts a moderate increase of  $R$  with  $Q^2$  in the DIS domain.

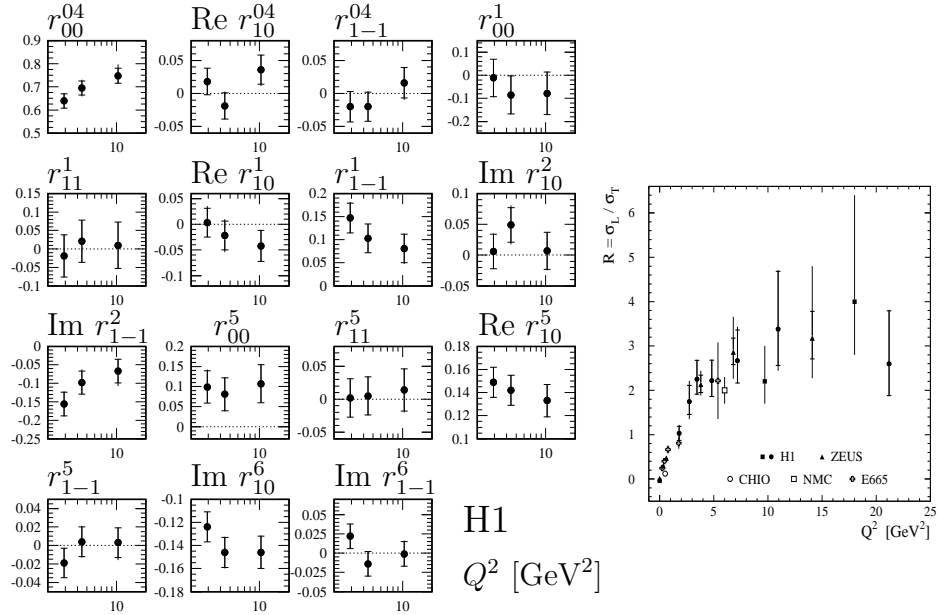


Figure 6: a) Spin density matrix elements for elastic electroproduction of  $\rho$  mesons as a function of  $Q^2$  <sup>30</sup>; the dashed lines indicate the expected null values in the case of SCHC. b) The ratio  $R$  of cross sections for elastic  $\rho$  meson electroproduction by longitudinal and transverse photons, as a function of  $Q^2$ .

It is also found <sup>30</sup> that the longitudinal and transverse amplitudes are nearly in phase ( $\cos \delta = 0.93 \pm 0.03$ ), assuming SCHC and natural parity exchange. This is similar to lower energy measurements <sup>6,36,38</sup>

A QCD based calculation <sup>23</sup> predicts for the amplitudes the hierarchy

$$|T_{\lambda\rho\lambda\gamma}| = |T_{00}| > |T_{11}| > |T_{01}| > |T_{10}| > |T_{1-1}|, \quad (3)$$

which is supported by the measurement of the matrix elements, and also the magnitude of the element  $r_{00}^5$  <sup>30,35</sup>.

Values of the matrix elements close to those for the  $\rho$  are obtained for  $\phi$  mesons<sup>35</sup>. For  $J/\psi$ , the ratio  $R$  of cross sections increases from values compatible with zero in photoproduction<sup>25,26</sup> to  $\approx 0.4$  for  $\langle Q^2 \rangle \simeq 4 \text{ GeV}^2$ <sup>29,28</sup>; this is smaller than for  $\rho$  production at the same  $\langle Q^2 \rangle$ , but is of the same order if compared at the same value of  $Q^2/m_V^2$ .

## 4 Other Features

### 4.1 VM Production Ratio

Predictions are obtained in pQCD for the cross section ratio of different VM production<sup>18,21</sup>. As apparent in eq. (2), this ratio is determined by the photon coupling to the  $q\bar{q}$  pairs, i.e. the charge of the quarks in the VM's, and the effects of the wave functions. For  $\phi/\rho$ <sup>16,31,39,40</sup>, the ratio increases with  $Q^2$  towards the value 2/9 obtained from quark counting (see Fig. 7a). For  $\psi/\rho$ , the ratio is about a factor 1/200 in photoproduction in the HERA energy range, but flavour symmetry is restored within a factor 2 for  $Q^2$  above 10  $\text{GeV}^2$ <sup>29,32</sup>.

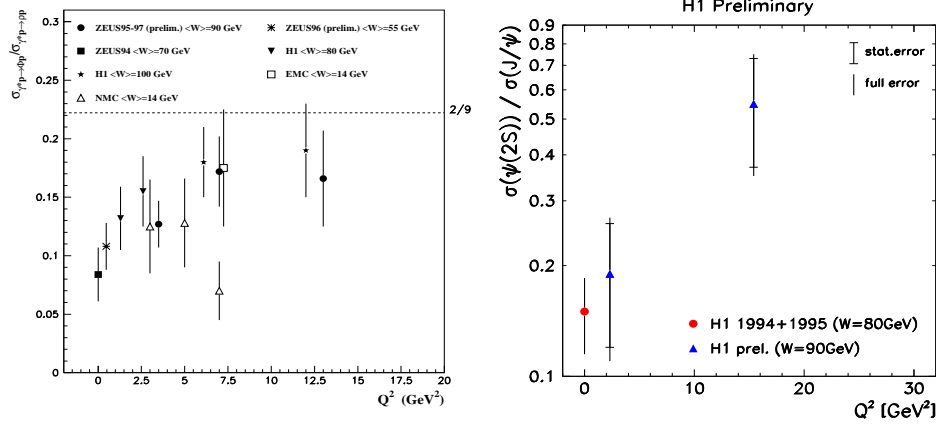


Figure 7: Ratio  $R$  of cross sections for a)  $\phi$  and  $\rho$ ; b)  $\psi(2s)$  and  $J/\psi$  meson production, as a function of  $Q^2$ .

The case of the  $\psi(2s)/\psi$  ratio illustrates the interesting phenomenon of the “scanning” of the VM wave function as  $Q^2$  varies. Because of the node in the  $\psi(2s)$  wave function, which induces approximately cancelling contributions in the production amplitude, the photoproduction of  $\psi(2s)$  mesons is small. As  $Q^2$  increases, the transverse size of the  $q\bar{q}$  pair decreases, thus avoiding the cancellation effect. The resulting increase with  $Q^2$  of the cross section ratio is illustrated in Fig. 7b<sup>28</sup>, the asymptotic limit being computed to be of the order of 0.5<sup>18,21</sup>.

## 4.2 Mass Distribution

For  $\rho$  photoproduction, the  $(\pi, \pi)$  mass distribution is distorted with respect to a (relativistic) Breit-Wigner distribution, with an excess of events at small masses and a deficit at large masses. This phenomenon, known as “skewing”, is attributed to the interference between resonant  $\rho$  production and non-resonant pion pair production, the interference changing sign at the resonance pole<sup>41</sup>. The skewing is observed to decrease in photoproduction as  $|t|$  increases<sup>14</sup> (see Fig. 8a). The skewing also decreases with increasing  $Q^2$  as seen in Fig. 8b for two different parameterisations<sup>41,42</sup>.

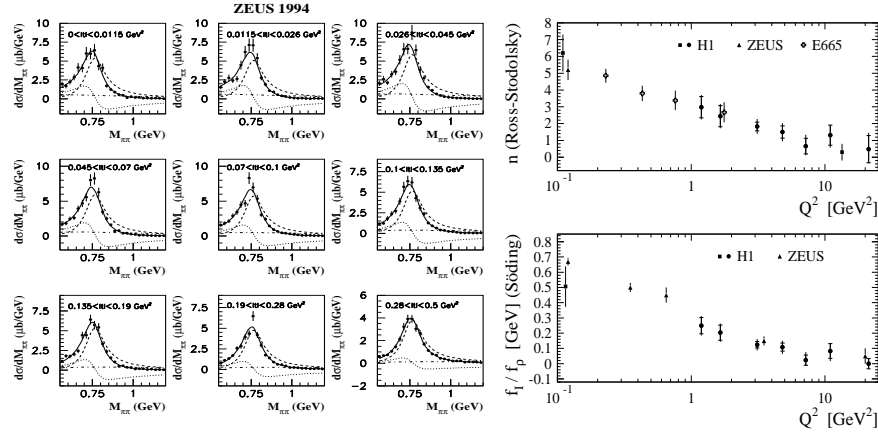


Figure 8: a) Mass distribution  $M_{\pi\pi}$  for  $\rho$  photoproduction, for different values of  $|t|$ <sup>14</sup>; the dashed curves represent the Breit-Wigner distribution, the dotted curves the interference with non-resonant pion pair, and the full curves the sum. b) Two parameterisations<sup>41,42</sup> of the skewing of the  $M_{\pi\pi}$  mass distribution for  $\rho$  production, as a function of  $Q^2$ <sup>8,11,14,12,29,30</sup>.

## 5 Conclusions

Abundant data have been collected at HERA on diffractive production of light and heavy vector mesons, in the presence of the scales  $Q^2$ ,  $m_q$  and  $t$ .

A strong energy dependence of the cross section is observed for  $J/\psi$  production; an indication is found for a similar behaviour for  $\rho$  mesons at high  $Q^2$ . In the light of perturbative QCD, with the pomeron modelled as a gluon pair, these features are interpreted as reflecting the strong increases of the gluon distribution in the proton at high energy, and quantitative agreement is reached for  $J/\psi$  production. The  $Q^2$  dependence of VM production is also qualitatively explained in pQCD approaches.

The ratio of the longitudinal to transverse photon cross sections for  $\rho$  production increases rapidly with  $Q^2$ , but this increase is non-linear for  $Q^2 \gtrsim 2$

GeV<sup>2</sup>. This behaviour has been reproduced recently by a model based on QCD. More generally, the full set of  $\rho$  meson spin density matrix elements has been measured. The correct hierarchy between scattering amplitudes and the magnitude of the dominant helicity-flip amplitude are also qualitatively reproduced in a QCD approach.

In summary, great progress has been made in the understanding of VM production at high energy when a hard scale is present ( $m_c$ ,  $Q^2$ ). This contributes significantly to the understanding of diffraction in a QCD framework.

### Acknowledgements

It is a pleasure to thank the organisers for a pleasant and fruitful Symposium, and my colleagues in H1 and ZEUS, in particular B. Clerbaux and P. Newmann, for numerous interesting discussions on diffraction.

### References

1. see e.g. P. Collins, *An Introduction to Regge Theory and High Energy Physics*, Cambridge Univ. Press, Cambridge (1977).
2. A. Donnachie and P.V. Landshoff, *Phys. Lett.* **B296** (1992) 227.
3. J.-R. Cudell, K. Kang and S. Kim, *Phys. Lett.* **B395** (1997) 311.
4. M. Derrick, these proceedings;  
P. Marage, *Diffraction at HERA, An Experimentalist's View*, Proc. of the LISHEP98 Conf., Rio de Janeiro, 1998, hep-ph/9810551
5. T.H. Bauer et al., *Rev. Mod. Phys.* **50** (1978) 261.
6. W.D. Shambroom et al., CHIO Coll., *Phys. Rev.* **D26** (1982) 1.
7. P. Amaudruz et al., NMC Coll., *Zeit. Phys.* **C54** (1992) 239;  
M. Arneodo et al., NMC Coll., *Nucl. Phys.* **B429** (1994) 503.
8. M. R. Adams et al., E665 Coll., *Zeit. Phys.* **C74** (1997) 237.
9. M. Derrick et al., ZEUS Coll., *Zeit. Phys.* **C63** (1994) 391.
10. S. Aid et al., H1 Coll., *Zeit. Phys.* **C69** (1995) 27.
11. M. Derrick et al., ZEUS Coll., *Zeit. Phys.* **C69** (1995) 39.
12. S. Aid et al., H1 Coll., *Nucl. Phys.* **463** (1996) 3.
13. M. Derrick et al., ZEUS Coll., *Zeit. Phys.* **C73** (1997) 253.
14. J. Breitweg et al., ZEUS Coll., *Eur. Phys. J.* **C2** (1998) 247.
15. M. Derrick et al., ZEUS Coll., *Zeit. Phys.* **C73** (1996) 73.
16. M. Derrick et al., ZEUS Coll., *Phys. Lett.* **B377** (1996) 259.
17. ZEUS Coll., *Study of Vector Meson Production at Large  $|t|$  at HERA and Determination of the Pomeron Trajectory*, Int. Conf. on HEP, Vancouver, Canada, 1998.

18. B.Z. Kopeliovich and B.G. Zakharov, *Phys. Rev.* **D44** (1991) 3466;  
B.Z. Kopeliovich et al., *Phys. Lett.* **B324** (1994) 469;  
J. Nemchik et al., *Phys. Lett.* **B341** (1994) 228.
19. M. Ryskin, *Zeit. Phys.* **C57** (1993) 89;  
M. Ryskin et al., *Zeit. Phys.* **C76** (1997) 231.
20. S.J. Brodsky et al., *Phys. Rev.* **D50** (1994) 3134.
21. L. Frankfurt, W. Koepf and M. Strikman, *Phys. Rev.* **D54** (1996) 3194;  
*Phys. Rev.* **D57** (1998) 512.
22. A.D. Martin, M. Ryskin and T. Teubner, *Phys. Rev.* **D55** (1997) 4329.
23. D.Yu. Ivanov and R. Kirschner, *Phys. Rev.* **D59** (1998) 114026.
24. I. Royen and J.-R. Cudell, *Fermi Motion and Quark Off-shellness in Elastic Vector-Meson Production*, hep-ph/9807294.
25. S. Aid et al., H1 Coll., *Nucl. Phys.* **472** (1996) 3.
26. J. Breitweg et al., ZEUS Coll., *Zeit. Phys.* **C75** (1997) 215.
27. H1 Coll., *Energy Dependence of the Cross Section for the Exclusive Photoproduction of  $J/\psi$  Mesons at HERA*, Int. Conf. on HEP, Vancouver, Canada, 1998.
28. H1 Coll., *Diffractional Charmonium Production in Deep-Inelastic Scattering at HERA*, Int. Conf. on HEP, Vancouver, Canada, 1998.
29. J. Breitweg et al., ZEUS Coll., *Eur. Phys. J.* **C6** (1999) 603.
30. C. Adloff et al., H1 Coll., DESY 99-010, subm. to *Eur. Phys. J.*
31. ZEUS Coll., *Exclusive Electroproduction of  $\phi$  Mesons at HERA*, Int. Conf. on HEP, Vancouver, Canada, 1998.
32. S. Aid et al., H1 Coll., *Nucl. Phys.* **468** (1996) 3.
33. H1 Coll., *Shrinkage in Exclusive  $J/\psi$  Photoproduction*, Int. Conf. on HEP, Vancouver, Canada, 1998.
34. K. Schilling and G. Wolf, *Nucl. Phys.* **B61** (1973) 381.
35. ZEUS Coll., *Angular distribution in exclusive electroproduction of  $\rho$  and  $\phi$  Mesons at HERA*, Int. Conf. on HEP, Vancouver, Canada, 1998.
36. P. Joos et al., *Nucl. Phys.* **B113** (1976) 53.
37. D. Schildknecht, G.A. Schuler and B. Surrow, *Vector-Meson Electroproduction from Generalized Vector Dominance*, hep-ph/9810370.
38. C. del Papa et al., *Phys. Rev.* **D19** (1979) 1303.
39. C. Adloff et al., H1 Coll., *Zeit. Phys.* **C75** (1997) 607.
40. H1 Coll., *Elastic Electroproduction of  $\rho$  and  $\phi$  Mesons for  $1 < Q^2 < 5$  GeV<sup>2</sup> at HERA*, Int. Europhys. Conf. on HEP, Jerusalem, Israel, 1997.
41. P. Söding, *Phys. Lett.* **B19** (1966) 702.
42. R. Ross and V. Stodolsky, *Phys. Rev.* **149** (1966) 1173.